

Why does surface ozone peak before a typhoon landing in southeast China?

Y. C. Jiang¹, T. L. Zhao¹, J. Liu^{2,3}, X. D. Xu⁴, C. H. Tan¹, X. H. Cheng⁵, X. Y. Bi^{6,7}, J. B. Gan⁸, J. F. You⁹, S. Z. Zhao¹⁰

¹ Collaborative Innovation Center on Forecast and Evaluation of Meteorological Disasters, Key Laboratory for Aerosol-Cloud-Precipitation of China Meteorological Administration, Nanjing University of Information Science and Technology, Nanjing 210044, China

² School of Atmospheric Sciences, Nanjing University, Nanjing, 210023, China

³ Department of Geography and Planning, University of Toronto, Toronto, M5S 3G3, Canada

⁴ State Key Laboratory of Severe Weather, Chinese Academy of Meteorological Sciences, Beijing 100081, China

⁵ Institute of Atmospheric Composition, Key Laboratory of Atmospheric Chemistry of China Meteorological Administration, Chinese Academy of Meteorological Sciences, Beijing 100081, China

⁶ State Key Laboratory of Atmospheric Boundary Layer Physics and Atmospheric Chemistry (LAPC), Institute of Atmospheric Physics, Chinese Academy of Sciences, Beijing, 100029, China

⁷ Institute of Tropical and Marine Meteorology/Guangdong Provincial Key Laboratory of Regional Numerical Weather Prediction, China Meteorological Administration, Guangzhou, 510080, China

⁸ Fujian Provincial Environmental Monitoring Center, Fuzhou 350003, China

⁹ Quanzhou Municipal Bureau of Meteorology, Quanzhou 361012, China

¹⁰ Xiamen Municipal Bureau of Meteorology, Xiamen 362000, China

Correspondence to: T. L. Zhao (tlzhao@nuist.edu.cn)

1

2 **Key Points**

- 3 • An O₃ episode with high nighttime O₃ was observed before typhoon landing
- 4 • The subsiding branches of TC circulation were identified to enhance surface O₃
- 5 • The STE of O₃ driven by the large scale TC can threaten to ambient air quality

6

7 **Abstract**

8 A high O₃ episode with the large increases in surface ozone by 21-42 ppbv and the nocturnal
9 surface O₃ levels exceeding 70 ppbv was observed in the region between Xiamen and
10 Quanzhou over the southeastern coast of China during June 12-14, 2014, before Typhoon
11 Hagibis landing. Variations in the surface O₃, NO₂, CO and meteorology during Typhoon
12 Hagibis event clearly suggest a substantial impact of the peripheral downdrafts in the large
13 scale typhoon circulation on such an O₃ episode with excluding the contributions of
14 photochemical production and the horizontal transport. The influence of vertical O₃ transport
15 from the upper troposphere and lower stratosphere (UTLS) region on high surface O₃ levels is
16 further confirmed by a negative correlation between surface O₃ and CO concentrations as well
17 as dry surface air observed during the O₃ episode. This study provides observational evidence
18 of typhoon-driven intrusion of O₃ from the UTLS region to surface air, revealing a significant
19 effect of such a process of stratosphere-troposphere exchange (STE) of O₃ on tropospheric O₃
20 and ambient air quality.

21 **Key words:** typhoon, ozone episode, vertical transport, stratosphere-troposphere exchange

22

23 **1 Introduction**

24 Tropospheric O₃, as an important chemical species with the effects of oxidation, toxicity and
25 greenhouse gas on climate and environment, is generated through a series of complex
26 photochemical reactions related to oxides of nitrogen (NO_x) and volatile organic compounds
27 (VOC) under strong solar radiation. Both strong local photochemical production and
28 atmospheric transport processes can lead to high surface O₃ concentrations (Jacob, 1999).
29 Weather condition can profoundly influence tropospheric O₃ levels through physical and

1 chemical processes and their interactions that modulate O₃ and its precursors (Huang et al.,
2 2005; Xue et al., 2014). The variation of tropospheric O₃ is largely influenced by the STE of
3 air mass and chemical species (Holton et al., 1995; Tang et al., 2011; Hsu and Prather, 2014).

4

5 A tropical cyclone (TC), as a large scale weather system with strong convection, is referred to
6 as a typhoon over the Western Pacific or a hurricane over the Northern Atlantic. A typical TC
7 can span a large radius of 100-2000 km with the vertical circulation of strong convection
8 extending into the UTLS region at heights of 10-18 km (Emanuel, 1986). A three-dimensional
9 TC circulation consists of the rotational air flow in the horizontal direction and the
10 in-up-out-down overturning flow in the vertical direction, along which air mass near the
11 surface can rise into thunderstorm clouds, outflowing at high levels in the UTLS and
12 subsiding in the periphery. As an important STE mechanism, the vertical TC circulation with
13 internal updrafts and peripheral downdrafts between the surface and the UTLS region exerts
14 an enormous impact on air mass and energy transports in the troposphere (Baray et al., 1998;
15 Fadnavis et al., 2011), as well as redistribution of tropospheric O₃ (Baray et al., 1999).

16

17 Air intrusions from the stratosphere to the troposphere were speculated to increase O₃
18 concentrations in the upper troposphere during a TC event (Bellevue et al., 2007). The uplift
19 flows of TC also transport O₃ from the surface to the middle and upper troposphere (Fadnavis
20 et al., 2011). Under the influence of frequent typhoon activities, O₃ episodes occurred over
21 coastal areas in southeast China (Feng et al., 2007; Wu et al., 2013). The stagnant
22 meteorological conditions with strong subsidence and stable stratification in the boundary
23 layer resulted in pollutant accumulations with high O₃ before typhoon landings over southeast
24 China (Feng et al., 2007). The peripheral O₃ was regionally transported by strong horizontal
25 typhoon winds (Huang et al., 2006).

26

27 Convection and orographic forcing can be important for the STE and the modification of trace
28 gases between the boundary layer and the free troposphere (Lelieveld and Crutzen, 1994;
29 Donnell et al., 2001; Weber and Prevot, 2002; Ding et al., 2009). O₃-rich air aloft could be
30 transported downward to the surface, when the cold front passage or nocturnal residual layer

1 “leaky” occurred (Hu et al., 2013a, 2013b). The near-surface O₃ levels abruptly increased due
2 to the downward O₃ transport from the free troposphere by tropical convections, enhancing O₃
3 levels in the boundary layer by as much as 20 to 30 ppbv (Betts et al. 2002; Sahu and Lal
4 2006; Grant et al. 2008). A recent modeling study (Hu et al., 2010) estimated that the
5 downward transport resulted in a 39% increase in the O₃ burden within the lower atmosphere
6 (<2 km) during a deep moist convection event over West Africa in August 2006. These studies
7 on downdrafts of O₃ to the surface level are mostly focused on the mesoscale convections in
8 the tropics. The extent to which these UTLS ozone enhancements reach the surface is poorly
9 characterized.

10
11 Redistribution of tropospheric O₃ by the TC circulation has been studied from the
12 perspectives of the STE of O₃, strong horizontal advection, and the stagnant meteorology for
13 O₃ accumulations in the boundary layer. In this study, we report a new finding on the O₃-rich
14 air downdrafts from the UTLS region to the surface driven by vertical typhoon circulation, as
15 the deep stratospheric intrusions elevating western US of surface O₃ to unhealthy levels can
16 be classified as “exceptional events” (Lin et al., 2015). We investigate the O₃ variation during
17 a TC event of Typhoon Hagibis over northwest Pacific on the basis of observations of the
18 surface air pollutants and meteorology in Xiamen and Quanzhou region (XQR) over the
19 southeastern coast of China (Fig. 1) in June 2014. This study presents observational evidence
20 of a surface O₃ episode caused by downward transport of O₃ in the subsiding branches of
21 vertical TC circulation. this finding may shed some light on the function of downward O₃
22 transport from the UTLS regions in modulating O₃ in the lower troposphere with implications
23 of the STE on air quality and climate changes.

24 25 **2 Data and Observation**

26 The XQR area, a prefecture of Fujian Province, located in the western coast of Taiwan Strait,
27 southeast China (Fig. 1). The air quality data (<http://air.epmap.org/>), including surface
28 concentrations of O₃, nitrogen dioxide (NO₂) and carbon monoxide (CO), were measured at 8
29 environmental monitoring stations over XQR in June, 2014. The surface observations of wind,
30 air temperature, air pressure and relative humidity at the observatory of Xiamen (24.48°N,
31 118.07°E) were collected for meteorological analysis during Typhoon Hagibis in June 2014.

1 The FNL meteorological data in a horizontal resolution of $1^\circ \times 1^\circ$ with 27 vertical levels from
2 NCEP (National Centers for Environmental Prediction, USA) are used to describe the
3 circulations of Typhoon Hagibis.

4

5 Typhoon Hagibis, as a summertime TC over the northwest Pacific, was intensified into a
6 strong tropical storm over the South China Sea at Dongsha islands (116.8°E , 20.6°N) and then
7 gradually pushed northwards up the southeastern coast of China. Typhoon Hagibis made
8 landfall in Shantou, a coastal site of Guangdong Province, south of XQR, at 16:50 June 15
9 (local time, same for hereinafter) with the maximum sustained winds of 23 m s^{-1} . Figures
10 2a-2c show the distributions of sea-level pressure and near-surface wind fields over the region
11 from southeast China to northwest Pacific at 14:00 June 13, 20:00 June 13 and 20:00 June 15,
12 2014 respectively, before and after the typhoon landing in the southeastern coast of China.

13

14 The hourly surface O_3 concentrations over XQR during Typhoon Hagibis are shown in Figure
15 3a with a noticeable anomaly in O_3 concentrations before and after the typhoon landfall. XQR
16 was situated in the typhoon periphery when Typhoon Hagibis was located in South China Sea
17 during June 12-14, 2014 (Figs. 2a and 2b). A high O_3 episode occurred from the noon of June
18 12 to the afternoon of June 14. In particular, the nocturnal surface O_3 concentrations exceeded
19 70 ppbv from June 13 to 14, 2014 (Fig. 3c). The 8-hour averaged surface O_3 concentrations of
20 80 ppbv at Huli and Xidong (sites 5 and 6 in Fig. 1) in XQR reached the “hazardous” O_3 level
21 of the Chinese national standards for ambient air quality. The surface O_3 obviously decreased
22 over XQR when Typhoon Hagibis was closer to the landfall in southeast China on June 15,
23 2014 (Fig. 2c). By using the hourly O_3 measurement data over XQR, the normal and
24 anomalous patterns of diurnal O_3 changes could be represented by the surface O_3 averages
25 over June 2014 excluding 12–14 June and over 12–14 June 2014 respectively (Fig. 3d). It is
26 shown in Figure 3d that the normal surface O_3 levels over XQR in June 2014 shifted diurnally
27 from 17 ppbv at 2:00 to 52 ppbv at 14:00 with a daily O_3 mean of about 30 ppbv, while the
28 anomalously high surface O_3 levels during the O_3 episode varied between nighttime 51 ppbv
29 and daytime 70 ppbv with an O_3 mean of about 57 ppbv. Comparing to the normal O_3 levels in
30 June 2014, the averaged enhancements of surface O_3 by about 21 ppbv in daytime and up to
31 42 ppbv in nighttime over XQR are estimated for the O_3 episode before Typhoon Hagibis

1 landing.

2

3 **3 Analysis and Discussion**

4 The surface O₃ variation is complex, resulted from interactions of chemical production and
5 dynamic transport on different scales (Jacob, 1999). In the following we examine this case of
6 surface O₃ peak before a typhoon landing in southeast China from chemical production,
7 horizontal advection and vertical transport.

8

9 Tropospheric O₃ is formed through a series of complex photochemical reactions of NO_x and
10 VOC under strong solar radiation. The O₃ concentrations in suburban and rural areas are
11 usually most sensitive to NO_x variations (Chameides et al., 1992; Duncan and Chameides,
12 1998). Notably, the surface NO₂ levels kept around 10 ppbv during the O₃ episode from June
13 12 to 14, almost the same as normal NO₂ levels during non-polluted days (Figs. 3b and 3c). In
14 particularly high O₃ levels anomalously persisted in the night without photochemical reaction.
15 Photochemical production could not be speculated to determine the high O₃ episode.
16 Furthermore, any obvious increases in surface air temperature were not observed for strong
17 photochemical reactions for such high O₃ production during the episode of June 12-14 in
18 XQR (Fig. 4a), since air temperature could represent the solar radiation conditions during
19 summertime. The weather over the XQR region was characterized by the clear sky, strong
20 solar radiation, weak wind, and stable atmospheric boundary layer when TC is about 600 to
21 1000 km away during the O₃ episode of 12-14 June (Fig. 4). All these are the favorable
22 conditions for photochemical production of O₃, which is confirmed by the diurnal variation of
23 O₃ during the episode (Fig. 3d). However, a comparison of diurnal O₃ changes in June 2014
24 and during the O₃ episode (Fig. 3d) clearly presents the anomalies in the diurnal O₃ variation
25 over June 12-14, suggesting a less contribution of the local photochemical O₃ production to
26 the peak O₃.

27

28 During June 12-14, weak easterly winds over XQR (Fig. 2a, Fig. 4b) were observed to be
29 unfavorable for horizontal transport of O₃ and its precursors. The easterly wind could even
30 carry clean air from the Pacific Ocean to XQR. Moreover, the daily change of near-surface air

1 mass divergence over XQR clearly presented a shift of the negative to positive values for
2 convergence and divergence conditions during normal and high O₃ periods (Fig. 3b). The
3 near-surface air mass divergence (positive values in divergence in Fig. 4b) in association with
4 a high surface air pressure (Fig. 4c) over XQR suppressed the advection import O₃ and its
5 precursors towards XQR during the O₃ episode of June 12-14, 2014. The meteorological
6 conditions of easterly clean air from ocean and near-surface air divergence over XQR were
7 unfavorable to horizontal transport of air pollutants to XQR during the O₃ episode. Therefore,
8 the surface O₃ peak of June 12-14 before the typhoon landing was unlikely caused by
9 horizontal advection or transport of O₃ and its precursors.

10

11 Figures 5 presents the cross sections of vertical velocity along the lines from the typhoon
12 center to XQR (as shown in Fig. 2 with the black solid lines) at 14:00 and 20:00 June 13, as
13 well as 20:00 June 15, 2014 respectively. In accompany with the strong rising motions from
14 the surface up to the UTLS around 100 hPa near the typhoon center (Figs. 5a and 5b), the
15 subsiding branches of vertical typhoon circulation were located over XQR in the northeastern
16 periphery of Typhoon Hagibis at 14:00 and 20:00 June 13, 2014 (Figs. 2a and 5a, Figs. 2b and
17 5b). A typical structure of TC circulation with the in-up-out-down overturning flows in the
18 vertical direction built up the internal updrafts and peripheral downdrafts for air mass
19 exchange between the surface level and the UTLS region (Figs. 5a-5b). The well-organized
20 deep and strong downdrafts occurred over XQR during this episode before the typhoon
21 landfall with the subsiding velocity exceeding 20 Pa s⁻¹ at 14:00 and 20:00 in June 13. As
22 Typhoon Hagibis approached and landed the coast in southeast China (Fig. 2), the downdrafts
23 were changed to the updrafts over XQR on June 15 (Fig. 5c), and the surface O₃
24 concentrations dropped to the normal levels over XQR (Fig. 3a).

25

26 A climatological pattern of vertical O₃ distribution presents the uniquely elevated O₃
27 concentrations in the UTLS region (Liu et al., 2013). The large scale convections of Typhoon
28 Hagibis were fully developed and well organized with strong uplifts reaching to the UTLS
29 around 100hPa and consecutively downward flows to the surface level over XQR (Figs.
30 5a-5b), which could efficiently deliver O₃-rich air from the UTLS region to the surface
31 leading to the surface O₃ enhancement by about 27 ppbv in daytime and up to 40 ppbv in

1 nighttime observed over XQR during June 12-14 (Figs. 3c-3d). Furthermore, low relative
2 humidity and high air pressure on the XQR surface during June 12-14 (Figs. 4c and 4d) add
3 evidences for the strong downward transport of O₃ in the subsiding branches of TC with dry
4 air mass of the UTLS region affecting the surface air, given that surface relative humidity
5 dropped sharply (Fig. 4d) and air temperature decreased slightly (Fig. 4a) over XQR during
6 June 12-14. Therefore, it is the downdrafts of O₃-rich air from the UTLS that played a
7 decisive role in the formation of O₃ episode before a typhoon landing in southeast China.

8

9 The correlation between O₃ and CO has been widely used to identify sources of tropospheric
10 O₃. When O₃ and CO are positively correlated, O₃ is usually originated from the
11 anthropogenic sources with photochemical reactions (Parrish et al., 1998; Voulgarakis et al.,
12 2011). A negative correlation of O₃ and CO generally indicates the vertical O₃ transport from
13 the upper atmosphere, where air is poor in CO but rich in O₃ (Moody et al., 1995; Parrish et
14 al., 1998). The correlations between hourly CO and O₃ concentrations measured at 8 sites in
15 XQR are shown over two periods from 12:00 June 11 to 12:00 June 12 and from 12:00 June
16 13 to 12:00 June 14, respectively (Fig. 6). In contrast to a significantly positive correlation of
17 the CO and O₃ during the first period, reflecting a dominant role of anthropogenic sources in
18 the O₃ changes (Fig. 6a), the CO and O₃ concentrations were negatively correlated
19 (significantly at P<0.005) during the second period (Fig. 6b), further confirming that the O₃
20 episode with nocturnal high O₃ over XQR was largely contributed by downward transport of
21 O₃-rich air in the peripheral subsidence of Typhoon Hagibis. For interpreting the enhanced
22 CO concentrations during the O₃ episode (Figs. 6a and 6b), we may consider the atmospheric
23 removal of CO by hydroxyl radical (OH). It is well-known that O₃ photolysis produces O¹d,
24 which react with H₂O to produce 2OH, and the reaction of CO with OH forms the stable end
25 product of carbon dioxide (CO₂) (Seinfeld and Spyros, 2006). In the situation of normal
26 photochemical production (Fig. 6a), high O₃ could lead to more OH production and
27 consequently lower CO. In the situation of peripheral O₃-rich air subsidence of the typhoon,
28 the downward dry air (Fig. 4d) with lower abundance of OH radicals could decrease the
29 removal of CO. This would result in CO accumulation and consequently high CO
30 concentrations, and high CO accumulation within boundary layer could overwhelm the
31 dilution of CO-poor air from the UTLS during the high O₃ episode.

1
2
3
4
5
6
7
8
9
10
11
12
13
14
15
16
17
18
19
20
21
22
23
24
25
26
27
28
29
30

4 Summary

This observation study presents an O₃ episode due to downward transport from the UTLS to surface air in the peripheral TC subsidence over the southeastern coast of China. A high O₃ event during June 12-14, 2014 was observed with the nocturnal surface O₃ levels exceeding 70 ppbv and large enhancements of surface O₃ concentrations by about 21 ppbv in daytime and up to 42 ppbv in nighttime. The ground observations of O₃, NO₂ and CO accompanying meteorology from both observations and reanalysis over XQR during the event of Typhoon Hagibis are examined to assess the contributions of chemical production, horizontal advection and vertical transport to the O₃ episode.

As the contributions of horizontal advection and chemical production to surface O₃ enhancement in the O₃ episode are excluded, the peripheral subsiding branches in the TC circulation bringing O₃-rich air from the UTLS to surface air are identified to be responsible for peaking the surface O₃ levels over the southeastern coast of China during June 12-14, 2014 before the landfall of Typhoon Hagibis. This rational analysis is further supported by a significantly negative correlation between the surface O₃ and CO as well as the dry surface air observed during the O₃ episode.

This case study of Typhoon Hagibis provides observational evidence of TC-driven vertical transport of O₃ from the UTLS region to the surface, revealing a significant effect of such a process of STE of O₃ on deterioration of air quality. Evidence suggests deep stratospheric intrusions can elevate surface O₃ to unhealthy levels before a typhoon landing in southeast China. Stratospheric O₃ is a natural source dominating tropospheric O₃ pollution in this scenario. Considering the frequency and distribution of TC in the world and their impact on STE, this finding has implications on tropospheric O₃ as well as environment and climate changes. Tropical cyclones, as an important STE mechanism, could exert an enormous impact on air mass and energy transports in the troposphere, as well as redistribution of tropospheric ozone.

1 A pattern of well-organized deep TC convection for the exchange of chemical species
2 between the UTLS and surface air is depicted in this case study of TC in southeast China.
3 Based on the understanding of the dynamical structure of TC and the chemical distribution in
4 the atmosphere, the strong subsiding branches of vertical TC circulation could unusually
5 transport the upper O₃-rich air to the surface in any TC events, which is to be further studied
6 with more comprehensive observations to characterize the extent to which these UTLS ozone
7 enhancements reach the surface. The implications of this finding on environment and climate
8 changes need to be explored by using coupled meteorology-chemistry models.

9

10 **Acknowledgements**

11 This work was jointly funded by National Science and Technology Project of China
12 (2014BAC22B04), the Key Basic Research Program of China (2014CB441203), the Science
13 and Technology Support Program of Jiangsu Province, China (BE2012771), and National
14 Natural Science Foundation of China (40906023). The air quality data were obtained freely
15 from the Chinese Ministry of Environmental Protection (<http://air.epmap.org/>). The
16 NCEP-FNL meteorological data were freely downloaded from the NOAA-CIRES Climate
17 Diagnostics Center, Boulder, Colorado, USA (<http://rda.ucar.edu/datasets/>).

18

19 **References**

- 20 Baray, J. L., Ancellet, G., Taupin, F. G., Bessafi, M., Baldy, S., and Keckhut, P.: Subtropical
21 tropopause break as a possible stratospheric source of ozone in the tropical troposphere, *J.*
22 *Atmos. Sol-Terr. Phy.*, 60(1), 27-36, doi:10.1016/S1364-6826(97)00116-8, 1998.
- 23 Baray, J. L., Ancellet, G., Randriambel, T., and Baldy, S.: Tropical cyclone Marlene and
24 stratosphere-troposphere exchange, *J. Geophys. Res.*, 104(D11), 13953-13970,
25 doi:10.1029/1999JD900028, 1999.
- 26 Bellevue, J., Baray, J. L., Baldy, S., Ancellet, G., Diab, R. D., and Ravetta, F.: Simulations of
27 stratospheric to tropospheric transport during the tropical cyclone Marlene event, *Atmos.*
28 *Environ.*, 41(31), 6510-6526, doi:10.1016/j.atmosenv.2007.04.040, 2007.
- 29 Betts, A. K., Gatti, L. V., Cordova, A. M., Silva Dias, M. A. F., and Fuentes, J. D.: Transport

1 of ozone to the surface by convective downdrafts at night, *J. Geophys. Res.*, 107(D20),
2 8046, doi:10.1029/2000JD000158, 2002.

3 Chameides, W. L., Fehsenfeld, F., Rodgers, M. O., Cardelino, C., Martinez, J., Parrish, D.,
4 Lonneman, W., Lawson, D. R., Rasmussen, R. A., Zimmerman, P., Greenberg, J.,
5 Middleton, P., and Wang, T.: Ozone precursors relationships in the ambient atmosphere, *J.*
6 *Geophys. Res.*, 97(D5), 6037-6055, doi:10.1029/91JD03014, 1992.

7 Ding, A., Wang, T., Xue, L., Stohl, A., Lei, H., Jin, D., Ren, Y., Wang, X., Wei, X., Qi, Y., Liu,
8 J., and Zhang, X.: Transport of north China air pollution by midlatitude cyclones: Case
9 study of aircraft measurements in summer 2007, *J. Geophys. Res.*, 114(D8), D08304,
10 doi:10.1029/2008JD011023, 2009.

11 Donnell, E. A., Fish, D. J., Dicks, E. M., and Thorpe, A. J.: Mechanisms for pollutant
12 transport between the boundary layer and the free troposphere, *J. Geophys. Res.*, 106(D8),
13 7847-7856, doi:10.1029/2000JD900730, 2001.

14 Duncan, B. N., and Chameides, W. L.: Effects of urban emission control strategies on the
15 export of ozone and ozone precursors from the urban atmosphere to the troposphere, *J.*
16 *Geophys. Res.*, 103(D21), 28159-28179, doi:10.1029/98JD02145, 1998.

17 Emanuel, K. A.: An air-sea interaction theory for tropical cyclones. Part I: steady-state
18 maintenance, *J. Atmos. Sci.*, 43(6), 585-605,
19 doi:10.1175/1520-0469(1986)043<0585:AASITF>2.0.CO;2, 1986.

20 Fadnavis, S., Berg, G., Buchunde, P., Ghude, S. D., and Krishnamurti, T. N.: Vertical transport
21 of ozone and CO during super cyclones in the Bay of Bengal as detected by Tropospheric
22 Emission Spectrometer, *Environ. Sci. Pollut. Res.*, 18(2), 301-315,
23 doi:10.1007/s11356-010-0374-3, 2011.

24 Feng, Y., Wang, A., Wu, D., and Xu, X.: The influence of tropical cyclone Melor on PM₁₀
25 concentrations during an aerosol episode over the Pearl River Delta region of China:
26 Numerical modeling versus observational analysis, *Atmos. Environ.*, 41(21), 4349-4365,
27 doi:10.1016/j.atmosenv.2007.01.055, 2007.

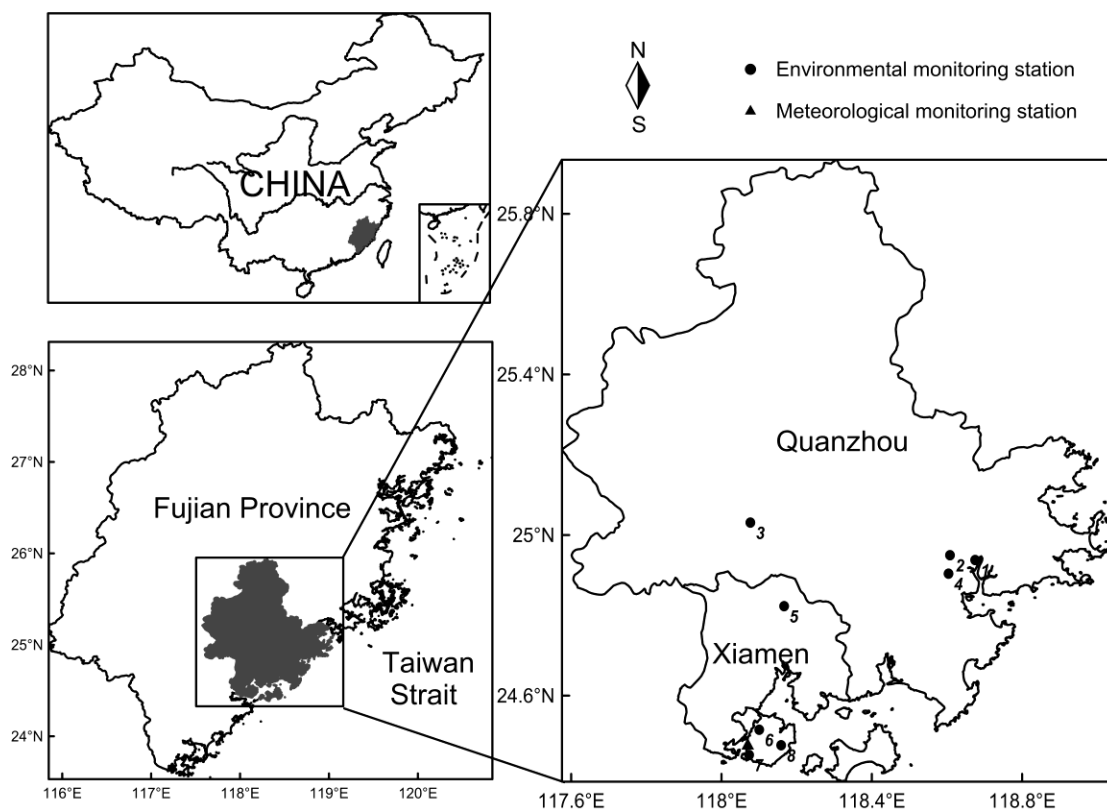
28 Grant, D. D., Fuentes, J. D., DeLonge, M. S., Chan, S., Joseph, E., Kucera, P., Ndiaye, S. A.,
29 and Gaye, A. T.: Ozone transport by mesoscale convective storms in western Senegal,
30 *Atmos. Environ.* 42(30), 7104-7114, doi:10.1016/j.atmosenv.2008.05.044, 2008.

- 1 Holton, J. R., Haynes, P. H., McIntyre, M. E., Douglass, A. R., Rood, R. B., and Pfister, L.:
2 Stratosphere-troposphere exchange, *Rev. Geophys.*, 33(4), 403-439, 1995.
- 3 Hsu, J., and Prather, M. J.: Is the residual vertical velocity a good proxy for
4 stratosphere-troposphere exchange of ozone?, *Geophys. Res. Lett.*, 41, 9024–9032,
5 doi:10.1002/2014GL061994, 2014.
- 6 Hu, X. M., Fuentes, J. D., and Zhang, F.: Downward transport and modification of
7 tropospheric ozone through moist convection, *J. Atmos. Chem.*, 65(1), 13-35,
8 doi:10.1007/s10874-010-9179-5, 2010.
- 9 Hu, X. M., Klein, P. M., Xue, M., Shapiro, A., and Nallapareddy, A.: Enhanced vertical
10 mixing associated with a nocturnal cold front passage and its impact on near-surface
11 temperature and ozone concentration, *J. Geophys. Res.*, 118(7), 2714-2728,
12 doi:10.1002/jgrd.50309, 2013.
- 13 Hu, X. M., Klein, P. M., Xue, M., Zhang, F., Doughty, D. C., Forkel, R., Joseph, E., and
14 Fuentes, J. D.: Impact of the vertical mixing induced by low-level jets on boundary layer
15 ozone concentration, *Atmos. Environ.*, 70, 123-130, doi:10.1016/j.atmosenv.2012.12.046,
16 2013.
- 17 Huang, J. P., Fung, C. H., Lau, K. H., and Qin, Y.: Numerical simulation and process analysis
18 of typhoon-related ozone episodes in Hong Kong, *J. Geophys. Res.*, 110(D5), D05301,
19 doi:10.1029/2004JD004914, 2005.
- 20 Huang, J. P., Fung, C. H., and Lau, K. H.: Integrated processes analysis and systematic
21 meteorological classification of ozone episodes in Hong Kong, *J. Geophys. Res.*, 111(D20),
22 D20309, doi:10.1029/2005JD007012, 2006.
- 23 Jacob, D. J. (1999), *Introduction of Atmospheric Chemistry*, pp. 234–243, Princeton Univ.
24 Press, Princeton, N. J..
- 25 Lelieveld, J. and Crutzen, P. J.: Role of deep cloud convection in the ozone budget of the
26 troposphere, *Science*, 264,793-797, 1994.
- 27 Lin, M., Fiore, A. M., Horowitz, L. W., Langford, A. O., Oltmans, S. J., Tarasick, D., and
28 Rieder, H. E.: Climate variability modulates western US ozone air quality in spring via
29 deep stratospheric intrusions, *Nature*, 6, 7105, doi:10.1038/ncomms8105, 2015.

- 1 Liu, J., Tarasick, D. W., Fioletov, V. E., McLinden, C., Zhao, T., Gong, S., Sioris, C., Jin, J. J.,
2 Liu, G., and Moeini, O.: A global ozone climatology from ozone soundings via trajectory
3 mapping: a stratospheric perspective, *Atmos. Chem. Phys.*, 13, 11441-11464,
4 doi:10.5194/acp-13-11441-2013, 2013.
- 5 Moody, J. L., Oltmans, J., and Merrill, T.: Transport climatology of tropospheric ozone:
6 Bermuda, 1988–1991, *J. Geophys. Res.*, 100(D4), 7179-7194, doi:10.1029/94JD02830,
7 1995.
- 8 Parrish, D. D., Trainer, M., Holloway, J. S., Yee, J. E., Warshawsky, M. S., Fehsenfeld, F. C.,
9 Forbes, G. L., and Moody, J. L.: Relationships between ozone and carbon monoxide at
10 surface sites in the North Atlantic region, *J. Geophys. Res.*, 103(D11), 13357-13376, 1998.
- 11 Sahu, L. K., and Lal, S.: Changes in surface ozone levels due to convective downdrafts over
12 the Bay of Bengal. *Geophys. Res. Lett.* 33(10), L10807, doi:10.1029/2006GL025994,
13 2006.
- 14 Seinfeld, J. H., and Spyros, N. P.: *Atmospheric Chemistry and Physics: From Air Pollution to*
15 *Climate Change*, 2nd edition, J. Wiley, New York, 2006.
- 16 Tang, Q., Prather, M. J., and Hsu, J.: Stratosphere - troposphere exchange ozone flux related
17 to deep convection, *Geophys. Res. Lett.*, 38, L03806, doi:10.1029/2010GL046039, 2011.
- 18 Voulgarakis, A., Telford, P. J., Aghedo, A. M., Braesicke, P., Faluvegi, G., Abraham, N. L.,
19 Bowman, K. W., Pyle, J. A., and Shindell, D. T.: Global multi-year O₃-CO correlation
20 patterns from models and TES satellite observations, *Atmos. Chem. Phys.*, 11, 5819-5838,
21 doi:10.5194/acp-11-5819-2011, 2011.
- 22 Weber, R. O., and Prevot, A. S. H.: Climatology of ozone transport from the free troposphere
23 into the boundary layer south of the Alps during North Foehn, *J. Geophys. Res.*, 107(D3),
24 4030, doi:10.1029/2001JD000987, 2002.
- 25 Wu, M., Wu, D., Fan, Q., Wang, B. M., Li, H. W., and Fan, S. J.: Observational studies of the
26 meteorological characteristics associated with poor air quality over the Pearl River Delta
27 in China, *Atmos. Chem. Phys.*, 13, 10755-10766, doi:10.5194/acp-13-10755-2013, 2013.
- 28 Xue, L. K., Wang, T., Gao, J., Ding, A. J., Zhou, X. H., Blake, D. R., Wang, X. F., Saunders, S.
29 M., Fan, S. J., Zuo, H. C., Zhang, Q. Z., and Wang, W. X.: Ground-level ozone in four

1 Chinese cities: precursors, regional transport and heterogeneous processes, Atmos. Chem.
2 Phys., 14, 13175-13188, doi:10.5194/acp-14-13175-2014, 2014.

3



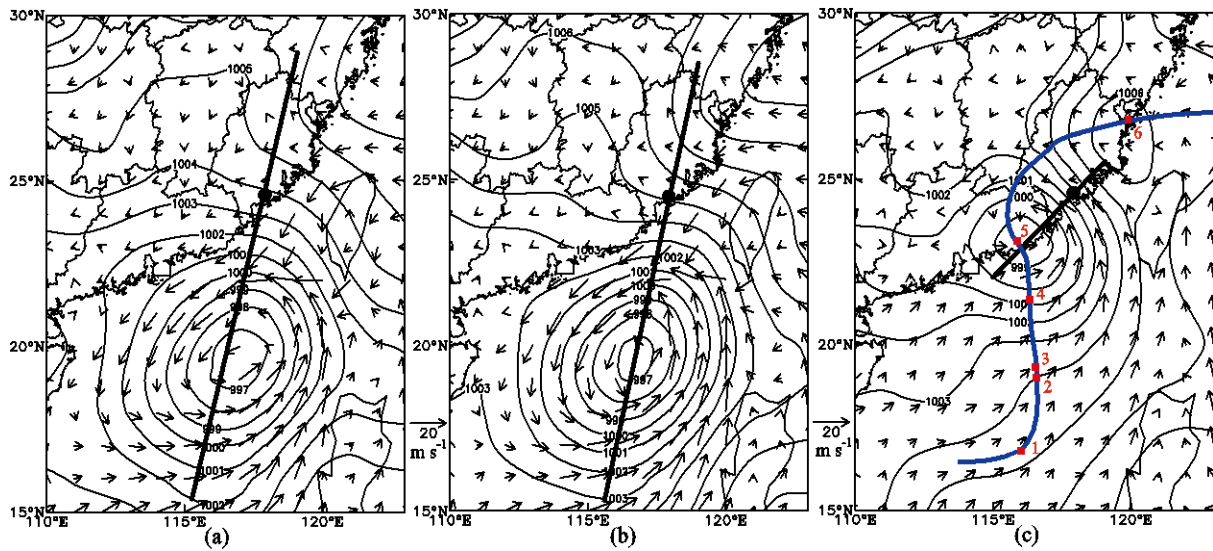
4

5

6 Figure 1. Locations of Fujian Province in China (shaded areas, upper left panel) and the
7 Xiamen and Quanzhou region (XQR) in Fujian Province (shaded areas, lower left panel), and
8 the distribution of 9 monitoring stations (8 environmental sites with black dots numbering
9 from 1 to 8, and 1 meteorological observatory of Xiamen with a black triangle) over XQR
10 (lower right panel).

11

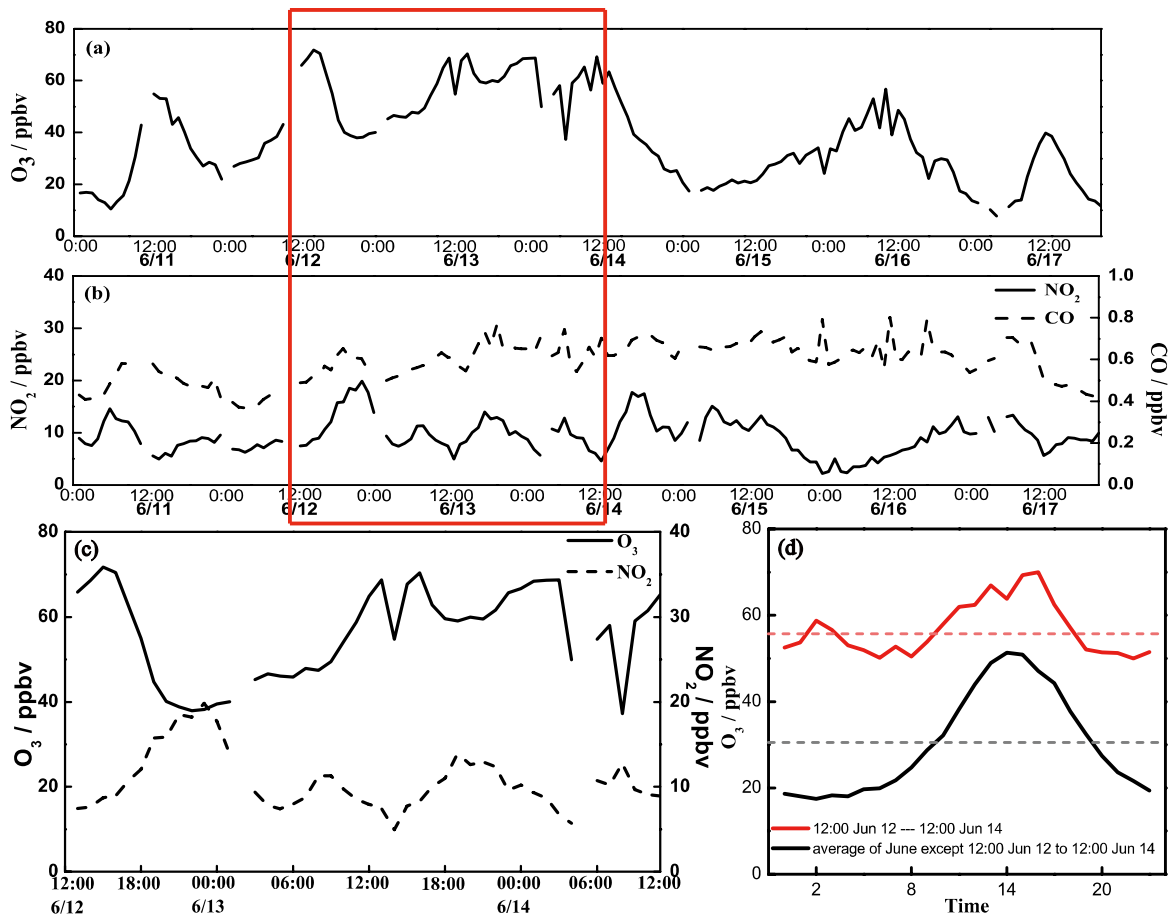
12



1

2 Figure 2. Sea-level air pressure (hPa, contour lines) and 1000 hPa wind vectors of
 3 NCEP-FNL data, at (a) 14:00 June 13, (b) 20:00 June 13 and (c) 20:00 June 15, 2014 with
 4 black dots representing XQR location. Three straight lines link XQR and the centers of
 5 Typhoon Hagibis. The blue curve with the red dots and numbers from 1 to 6 in (c) indicate the
 6 typhoon track with the typhoon locations of at 2:00 12 June, 14:00 13 June, 20:00 13 June,
 7 8:00 15 June, 20:00 15 June and 20:00 16 June respectively.

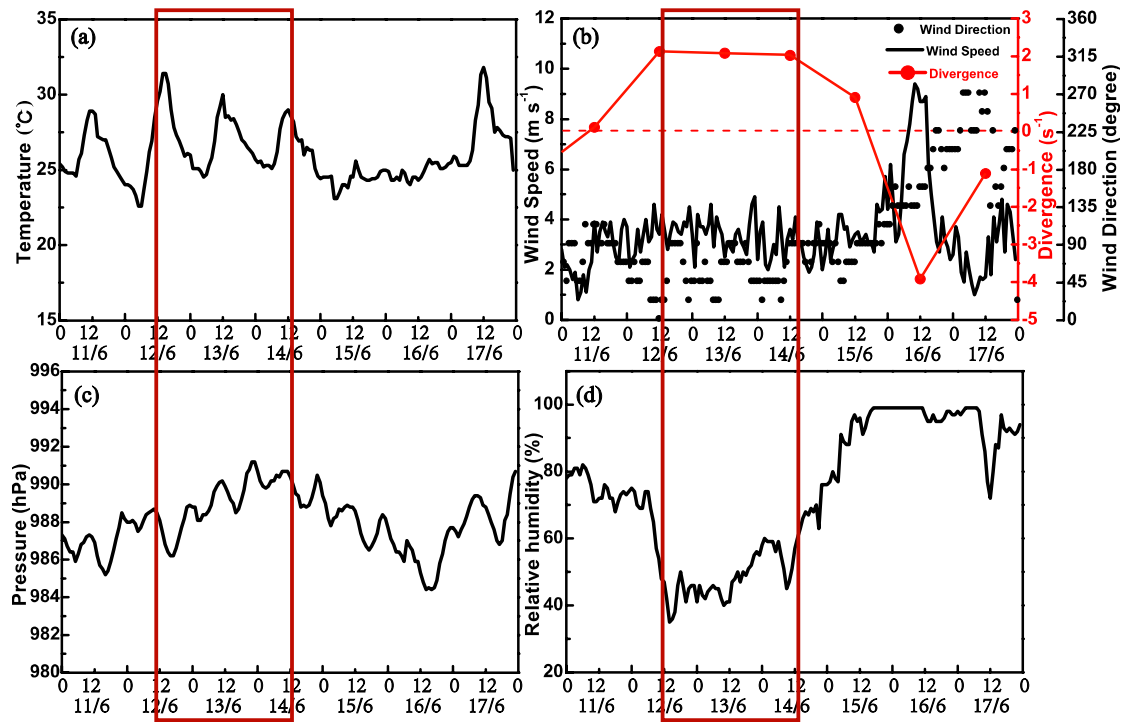
8



1

2 Figure 3. Hourly variations in the 8-site averaged surface concentrations of (a) O_3 , (b) NO_2
 3 during June 11-17 with the red rectangular column marking the period of surface O_3 event and
 4 (c) O_3 and NO_2 for the surface O_3 event over XQR, as well as (d) diurnal changes of surface
 5 O_3 from 12:00 Jun 12 to 12:00 Jun 14 (red curve) and in June excluding June 12-14, 2014
 6 (black curve) with two dotted lines indicating the daily averaged O_3 concentrations for two
 7 diurnal curves.

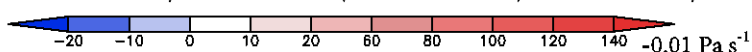
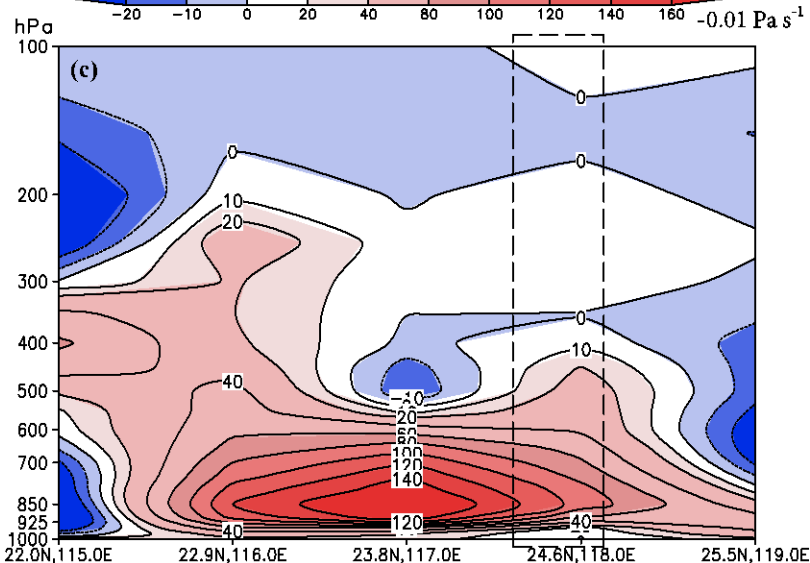
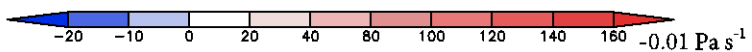
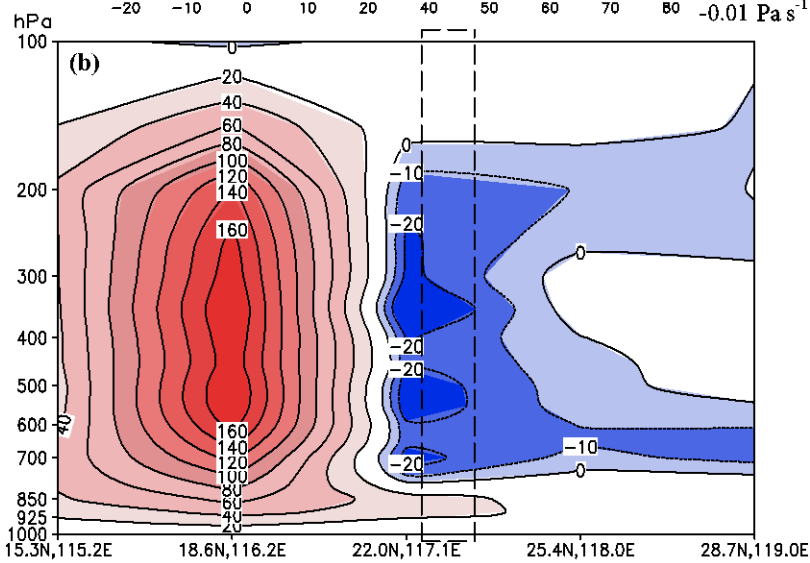
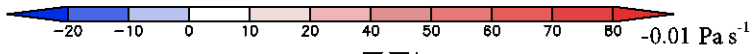
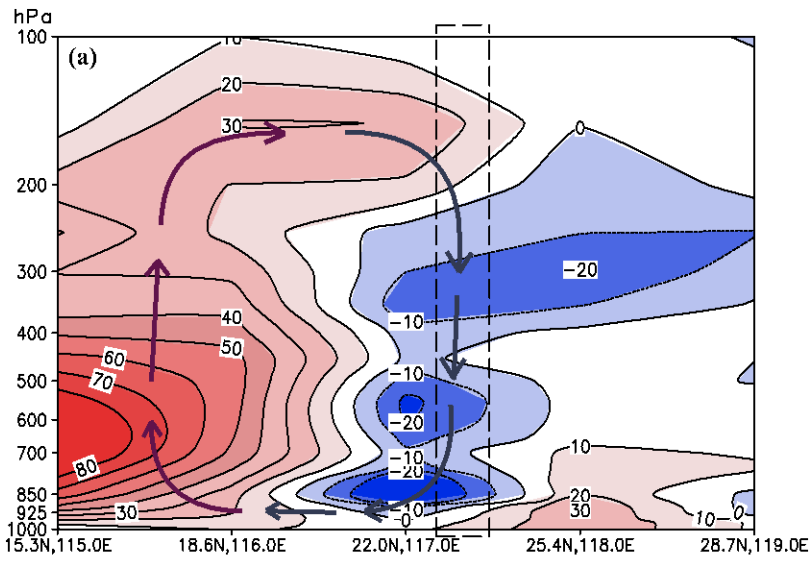
8



1

2 Figure 4. Time series of (a) surface air temperature (b) wind speed, direction and divergence,
 3 (c) air pressure and (d) relative humidity observed in the observatory of Xiamen from 11 to 17
 4 June 2014 with the red rectangular columns marking the period of surface O₃ event. The red
 5 curve in (b) is a daily variation in divergences at 1000 hPa over XQR, calculated with FNL
 6 data.

7

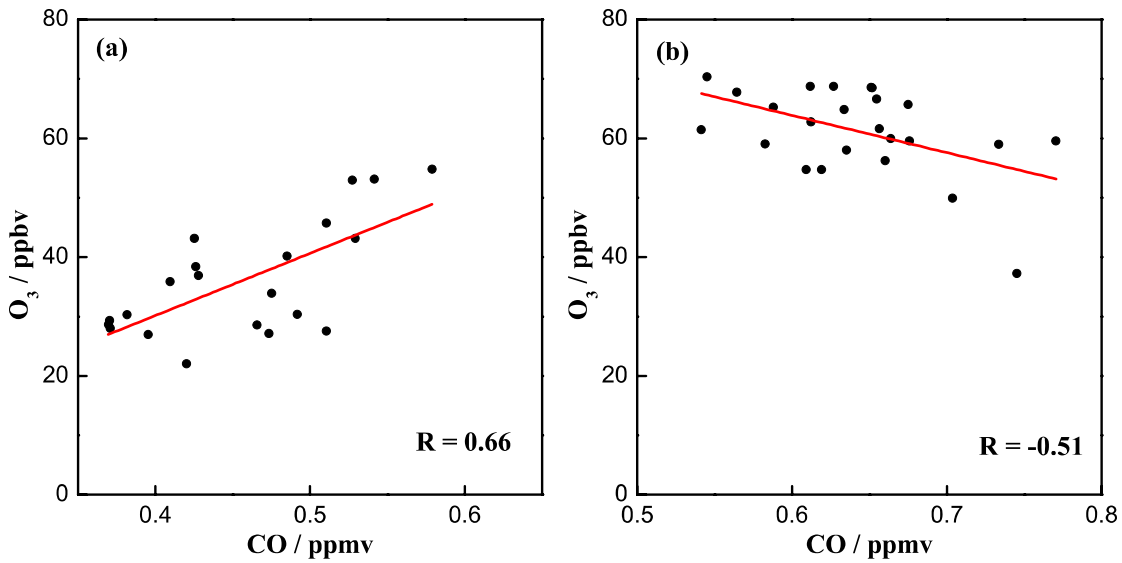


1

1

2 Figure 5. Vertical cross sections of vertical velocity (-0.01Pa s^{-1}) along the three straight
3 lines linking XQR and the centers of Typhoon Hagibis in Figure 2 at (a) 14:00 June 13, (b)
4 20:00 June 13 and (c) 20:00 June 15, 2014 (FNL data). Two dash boxes denote the location of
5 XQR. The lines with arrows indicate the in-up-out-down overturning air flows in the vertical
6 direction of typhoon.

7



8

9

10 Figure 6. Correlations between measured surface CO and O₃ over two periods respectively
11 (a) from 12:00 June 11 to 12:00 June 12 and (b) from 12:00 June 13 to 12:00 June 14, 2014,
12 passing the significant level of 0.005. Red lines are the linear fittings.